2022 17th International Conference on
Control, Automation, Robotics and Vision (ICARCV)
December 11-13, 2022. Singapore

Time-varying Quaternion Constrained Attitude Control Using Barrier Lyapunov Function

Srianish Vutukuri
Department of Aerospace Enginnering
Indian Institute of Science
Bengaluru, India
srianishv@iisc.ac.in

Arghya Chakravarty
Department of Aerospace Engineering
Indian Institute of Science
Bengaluru, India
arg.chakravarty@gmail.com

Radhakant Padhi
Department of Aerospace Engineering
Indian Institute of Science
Bengaluru, India
padhi@iisc.ac.in

2022 17th International Conference on Control, Automation, Robotics and Vision (ICARCV) | 978-1-6654-7687-4/22/$31.00 ©2022 IEEE | DOI: 10.1109/ICARCV57592.2022.10004348

***Abstract*—A novel, robust attitude controller for rigid bodies in the presence of time-varying orientation constraints is presented in this paper. Using an error transformation, the dynamic attitude constraints are converted into time-varying quaternion constraints. Subsequently, a robust attitude control law is synthesized using the backstepping philosophy in which barrier Lyapunov functions (BLFs) are used to achieve asymptotic tracking and simultaneously avoid attitude constraint violation. This is accomplished by ensuring the boundedness of BLFs in the closed-loop Lyapunov stability analysis. Besides the nominal scenario, an adaptive control law is also formulated to tackle moment of inertial uncertainties and an unknown, time-varying, bounded disturbance. In this case, the attitude tracking errors are uniformly ultimately bounded, whose bounds can be adjusted by user-defined constants. Note that in both scenarios, the dynamic attitude constraints are not transgressed. Finally, the effectiveness of the proposed controller is demonstrated by carrying out extensive numerical simulations in the presence of parametric uncertainties and disturbance torques.**

***Index Terms*—Attitude Control, Backstepping, Barrier Lyapunov Function, Constraints, Lyapunov Stability Analysis**

I. Introduction

The rigid body attitude control problem finds its application in several fields such as robot manipulators for industrial use, unmanned aerial vehicles / satellites for aerospace applications and laser systems / antennas for defense and communication. Quite often in such scenarios, tracking a reference attitude forms a fundamental requirement. To ensure safety during the tracking operation, the attitude of the rigid-body is subjected to dynamic constraints. Therefore, an effective attitude control law must ensure the non-violation of constraints during the entire tracking duration. In addition, the presence of parametric uncertainties as well as external disturbances pose an additional challenge while seeking for such a controller.

In the literature, the problem of constrained attitude control is being addressed along indirect optimal control [1], [2] and potential function [3], [4] based techniques. While indirect optimal control methods are effective in handling multiple attitude constraints, their implementation is often constrained by their computational complexity and real time performance. The potential function based methods are analytical, wherein, the attitude constraints are incorporated using artificial potential functions (APF). Subsequently, stabilizing attitude control laws that track the desired attitude and, at the same time, satisfy the orientation constraints are synthesized using Lyapunov based control techniques. However, it is to be noted that a majority of these techniques were utilized to synthesize controllers that are limited by their capability to handle static attitude constraints. Only recently, prescribed performance control [5], [6], which addresses a sub-class of the general time-varying attitude constraint problem was developed using barrier functions [7] and Lyapunov stability theory [8]. However, the dynamic error constraints were imposed on individual quaternion elements that fail to provide a physical intuition about the rigid-body attitude.

In this paper, the aforementioned limitations are tackled by synthesizing a robust, attitude controller by blending the philosophies of backstepping and barrier Lyapunov function (BLF) based state-constrained control design strategies. First, a set of cone angles [9] between the rigid-body and the desired reference frame are defined to be used as the attitude error variables. The cone angles represent a physically meaningful quantity to describe the attitude error between two reference frames. Next, an error transformation converts the dynamic constraints on the cone angles to time-varying, nonlinear quaternion constraints. Appropriate BLFs are constructed using the transformed variables and Lyapunov stability analysis via backstepping is performed to obtain an attitude control law that not only achieves asymptotic tracking but also ensures non-violation of attitude constraints. Besides the nominal scenario, an adaptive control law is also formulated to tackle moment of inertial uncertainties and an unknown, time-varying, bounded disturbance. In this case, the attitude tracking errors are uniformly ultimately bounded, whose bounds can be adjusted by user-defined constants. Note that in both scenarios, the dynamic attitude constraints are not transgressed. Finally, the effectiveness of the controller is demonstrated while tracking a moving reference frame in the presence of prescribed performance constraints on the attitude errors. On comparison with a controller designed using conventional quadratic lyapunov functions, the BLF based adaptive control law ensures robust attitude tracking and non-violation of constraints in the presence of various combinations of moment of inertia uncertainties and external disturbance torques.

II. Problem Formulation

A. Rigid Body Attitude Dynamics

Consider Fig. 1, which indicates the orientation of the rigid body-frame ($\mathcal{B}$) with respect to the inertial-frame ($\mathcal{I}$) using a unit quaternion ($\boldsymbol{q} = \left[\boldsymbol{q}_v^T \; q_4\right]^T$). The vector and scalar parts of the quaternion are given by $\boldsymbol{q}_v = [q_1 \; q_2 \; q_3]^T$ and q_4 respectively. The unit quaternion ($\boldsymbol{q}$) satisfies the constraint $\boldsymbol{q}_v^T \boldsymbol{q}_v + q_4^2 = 1$. Likewise, the orientation of the desired reference-frame ($\mathcal{R}$) with respect to the inertial-frame ($\mathcal{I}$) is indicated by a unit quaternion ($\boldsymbol{q}_r = \left[\boldsymbol{q}_{vr}^T \; q_{4r}\right]^T$) whose vector and scalar parts are represented by $\boldsymbol{q}_{vr} = [q_{1r} \; q_{2r} \; q_{3r}]^T$ and q_{4r} respectively. The relative orientation between the body-frame ($\mathcal{B}$) and the reference-frame ($\mathcal{R}$) is obtained using an error quaternion ($\boldsymbol{q}_e = \left[\boldsymbol{q}_{ve}^T \; q_{4e}\right]^T$) [10] whose vector and scalar components are computed as

$$\boldsymbol{q}_{ve} := [q_{1e} \; q_{2e} \; q_{3e}]^T = -q_4 \boldsymbol{q}_{vr} + q_{4r} \boldsymbol{q}_v + \boldsymbol{q}_v \times \boldsymbol{q}_{vr} \tag{1}$$

$$q_{4e} = q_4 q_{4r} + \boldsymbol{q}_v^T \boldsymbol{q}_{vr} \tag{2}$$

The angular velocity of $\mathcal{B}$ frame with respect to $\mathcal{I}$, expressed in $\mathcal{B}$ is $\boldsymbol{\omega}$. Similarly, angular velocity of $\mathcal{R}$ with respect to $\mathcal{I}$, expressed in $\mathcal{R}$ frame is $\boldsymbol{\omega}_r$. The relative angular velocity between $\mathcal{B}$ and $\mathcal{R}$ frames, expressed in $\mathcal{B}$ frame is $\boldsymbol{\omega}_e = [\omega_{1e} \; \omega_{2e} \; \omega_{3e}]^T$ and computed as

$$\boldsymbol{\omega}_e = \boldsymbol{\omega} - C_{\mathcal{R}}^{\mathcal{B}} \boldsymbol{\omega}_r \tag{3}$$

here, $C_{\mathcal{R}}^{\mathcal{B}}$ represents the direction cosine matrix that transforms a vector expressed in $\mathcal{R}$ frame to $\mathcal{B}$ frame and is computed using error quaternion ($\boldsymbol{q}_e$) [10] as

$$C_{\mathcal{R}}^{\mathcal{B}} = \left(q_{4e}^2 - \boldsymbol{q}_{ve}^T \boldsymbol{q}_{ve}\right) \boldsymbol{I}_{3\times3} + 2\boldsymbol{q}_{ve}\boldsymbol{q}_{ve}^T - 2q_{4e}\boldsymbol{q}_{ve}^{\times} \tag{4}$$

The attitude dynamics corresponding to the error quaternion ($\boldsymbol{q}_e$) as well as the relative angular velocity ($\boldsymbol{\omega}_e$) [10] is

$$\dot{\boldsymbol{q}}_e = Q_e \boldsymbol{\omega}_e \tag{5}$$

$$\dot{\boldsymbol{\omega}}_e = \dot{\boldsymbol{\omega}} + \boldsymbol{\omega}_e^{\times} C_R^B \boldsymbol{\omega}_r - C_R^B \dot{\boldsymbol{\omega}}_r \tag{6}$$

The matrix Q_e takes the form

$$Q_e = \frac{1}{2}\begin{bmatrix} q_{4e}\boldsymbol{I} + \boldsymbol{q}_{ve}^{\times} \\ -\boldsymbol{q}_{ve}^T \end{bmatrix}, \; \boldsymbol{q}_{ve}^{\times} = \begin{bmatrix} 0 & -q_{3e} & q_{2e} \\ q_{3e} & 0 & -q_{1e} \\ -q_{2e} & q_{1e} & 0 \end{bmatrix} \tag{7}$$

The angular velocity of the rigid body ($\boldsymbol{\omega}$) is manipulated by the application of a control torque ($\boldsymbol{\tau}_c$) in the presence of an unknown, time-varying, bounded disturbance torque ($\boldsymbol{\tau}_{ed}$) as

$$J\dot{\boldsymbol{\omega}} = -\boldsymbol{\omega}^{\times} J \boldsymbol{\omega} + \boldsymbol{\tau}_c + \boldsymbol{\tau}_{ed} \tag{8}$$

here, J indicates the moment of inertia matrix. In practice, J comprises of a known part (J_k) and a constant, unknown part (J_{uk}) related as $J = J_k + J_{uk}$.

B. Time-varying Attitude Constraints

As illustrated in Fig. 1, the cone angles δ_i between $\hat{b}_i$ and $\hat{r}_i$ axes for $i = 1, 2, 3$ indicate a way to quantify the orientation error between the $\mathcal{B}$ and $\mathcal{R}$ frames. While tracking the reference frame ($\mathcal{R}$), at any time, the cone angles corresponding to the three body-axes may be subjected to known time-varying constraints, i.e., $\delta_i(t) < \bar{\delta}_i(t)$. From now on-wards, the time dependence of δ_i and $\bar{\delta}_i$ is omitted for brevity, readability and convenience. To account for the time-varying attitude error constraints, an error transformation is applied to convert the angle constraints into appropriate quaternion constraints using the DCM (C_R^B) in (4) as

$$\hat{r}_1^T \hat{b}_1 = \cos(\delta_1) = 1 - 2q_{2e}^2 - 2q_{3e}^2 \tag{9}$$

The cone angle δ_1 in terms of the components of the error quaternion is obtained as

$$\delta_1 = \cos^{-1}(1 - 2q_{2e}^2 - 2q_{3e}^2) < \bar{\delta}_1 \tag{10}$$

From (10), the constraint on angle δ_1 is transformed into a constraint on the error quaternions as

$$e_1 := q_{2e}^2 + q_{3e}^2 < \bar{e}_1, \; \bar{e}_1 = \frac{1 - \cos(\bar{\delta}_1)}{2} \tag{11}$$

Similarly, the attitude errors along the remaining two axes written in terms of quaternion constraints are

$$e_2 := q_{1e}^2 + q_{3e}^2 < \bar{e}_2, \; \bar{e}_2 = \frac{1 - \cos(\bar{\delta}_2)}{2} \tag{12}$$

$$e_3 := q_{1e}^2 + q_{2e}^2 < \bar{e}_3, \; \bar{e}_3 = \frac{1 - \cos(\bar{\delta}_3)}{2} \tag{13}$$

The set of error quaternions ($\boldsymbol{q}_e$) that satisfy the constraints in (11), (12) and (13) form an inclusion type constraint set

$$\mathcal{U}_{q_e} := \{\boldsymbol{q}_e | \; e_i < \bar{e}_i \; \forall \; i = 1, 2, 3\} \tag{14}$$

From the above equations, it is straightforward to verify that when $\mathcal{B}$ frame is aligned to $\mathcal{R}$ frame, i.e., when the value of the error quaternion $\boldsymbol{q}_{ve} = \begin{bmatrix} q_{1e} & q_{2e} & q_{3e} \end{bmatrix}^T = \begin{bmatrix} 0 & 0 & 0 \end{bmatrix}^T$ and $q_{4e} = 1$, uniquely leads to $e_i = 0$ and $\delta_i = 0 \; \forall \; i = 1, 2, 3$, respectively.

Remark 1: At time t_0, without loss of generality, given the scalar error quaternion $q_{4e}(t_0) > 0$, tracking the desired frame ($\mathcal{R}$) via the shortest path warrants $q_{4e}(t) > 0$ for all $t > t_0$. Using (11), (12) and (13), the constraint set $\mathcal{U}_{q_e}$, in which the error quaternion evolves, that ensures the aforementioned statement must satisfy the following condition for all $t \geq t_0$

$$q_{1e}^2 + q_{2e}^2 + q_{3e}^2 < \frac{\bar{e}_1 + \bar{e}_2 + \bar{e}_3}{2} < 1 \tag{15}$$

Simplifying the right hand side of (15) results in the following inequality for constructing the cone angle constraints

$$\cos(\bar{\delta}_1) + \cos(\bar{\delta}_2) + \cos(\bar{\delta}_3) > -1 \tag{16}$$

Designing the output constraints $\bar{\delta}_i, \; i = 1, 2, 3$, such that (16) is satisfied, guarantees the possibility of the scalar error quaternion (q_{4e}) to take only positive values, i.e., ($q_{4e} > 0$) within the feasible set $\mathcal{U}_{q_e}$.

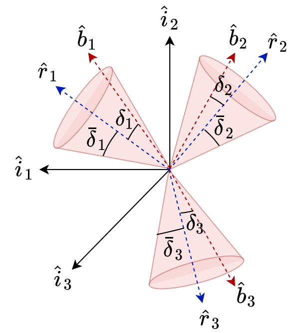

Figure 1: Body-frame ($\mathcal{B}$) tracking a reference-frame ($\mathcal{R}$).

C. Control Objective

To develop an adaptive controller, such that the following goals are achieved in the presence of moment of inertia uncertainity and a bounded, external disturbance torque.

1) Frame $\mathcal{B}$ tracks $\mathcal{R}$, i.e., $\boldsymbol{q}_e \to [0\ 0\ 0\ 1]^T$ and $\boldsymbol{\omega}_e \to \mathbf{0}_{3\times 1}$ and finally settles within a uniformly ultimately bounded set while strictly remaining within $\mathcal{U}_{q_e}$.
2) All signals in the closed-loop system remain bounded.

III. Preliminaries and Assumptions

Assumption 1: All the states viz., the quaternions and angular velocities are available for feedback control design.

Assumption 2: The initial cone angles strictly lie within the constraints, i.e., $\delta_i(t_0) < \bar{\delta}_i(t_0),\ i = 1, 2, 3$.

Assumption 3: The unknown external disturbance torque, $\boldsymbol{\tau}_{ed}$, is bounded, i.e., $\|\boldsymbol{\tau}_{ed}(t)\| < \bar{\tau}_{ed}$.

Lemma 1: [11] For any positive constant $k_z \in \mathbb{R}^+$, the following inequality holds for any $z \in [0, k_z)$

$$\log\left(\frac{k_z}{k_z - z}\right) \le \frac{z}{k_z - z} \tag{17}$$

Lemma 2: For a vector $\boldsymbol{x} \in \mathbb{R}^n$ and $\|\boldsymbol{x}\|_i$ representing the i^{th} norm, the following inequality always holds

$$\|\boldsymbol{x}\|_\infty \le \|\boldsymbol{x}\|_2 \le \|\boldsymbol{x}\|_1 \tag{18}$$

For a matrix $M \in \mathbb{R}^{n\times n}$, the following inequalities hold

$$\lambda_{\text{min}}(M)\boldsymbol{x}^T\boldsymbol{x} \le \boldsymbol{x}^T M\boldsymbol{x} \le \lambda_{\text{max}}(M)\boldsymbol{x}^T\boldsymbol{x} \tag{19}$$

$$\|M\boldsymbol{x}\|_2 \le \|M\|_2\|\boldsymbol{x}\|_2 \le \|M\|_F\|\boldsymbol{x}\|_2 \tag{20}$$

here, $\lambda_{\text{min}}(\bullet)$ and $\lambda_{\text{max}}(\bullet)$ denote the minimum and maximum eigenvalues of a matrix and $\|\bullet\|_F$ denotes the Forbenius norm. Given an two vectors $\boldsymbol{x}, \boldsymbol{y} \in \mathbb{R}^n$, then

$$(\boldsymbol{x} - \boldsymbol{y})^T(\boldsymbol{x} - \boldsymbol{y}) \ge 0 \tag{21}$$

Rearranging the above equation, leads to $\boldsymbol{x}^T\boldsymbol{y} \le \frac{\boldsymbol{x}^T\boldsymbol{x}}{2} + \frac{\boldsymbol{y}^T\boldsymbol{y}}{2}$

Lemma 3: [5] For any vector $\boldsymbol{x} = [x_1\ x_2\ x_3]^T \in \mathbb{R}^3$ and J representing the moment of inertia, there always exists a linear operator $L\{\bullet\} : \mathbb{R}^3 \to \mathbb{R}^{3\times 6}$ such that $J\boldsymbol{x} = \mathcal{L}\{\boldsymbol{x}\}\boldsymbol{\theta}$. The linear operator is defined as

$$\mathcal{L}\{\boldsymbol{x}\} := \begin{bmatrix} x_1 & x_2 & x_3 & 0 & 0 & 0 \\ 0 & x_1 & 0 & x_2 & x_3 & 0 \\ 0 & 0 & x_1 & 0 & x_2 & x_3 \end{bmatrix} \tag{22}$$

$$\boldsymbol{\theta} = \begin{bmatrix} J_{11} & J_{12} & J_{13} & J_{22} & J_{23} & J_{33} \end{bmatrix}^T \tag{23}$$

Lemma 4: [11] For a $\delta > 0$ and $x \in \mathbb{R}$, the following holds

$$0 \le |x| - x\tanh(x/\delta) \le \alpha\delta,\ \ \alpha = 0.2785 \tag{24}$$

IV. Controller Synthesis

A. Backstepping Design

A robust, adaptive control law is synthesized using the backstepping philosophy to achieve the objectives in II-C.

Step 1: As defined in (11), (12) and (13), four relevant output errors are chosen as e_1, e_2, e_3 and $e_4 = q_{4e} - 1$. Without loss of generality, with $q_{4e}(t_0) > 0$, defining the variable e_4 in the aforementioned manner prevents the unwinding issue, thereby tracking $\mathcal{R}$ via the shortest path. A Lyapunov function, V_q, is constructed as

$$V_q = \frac{k_q}{2}\left(\sum_{i=1}^{3}\log\left(\frac{\bar{e}_i}{\bar{e}_i - e_i}\right) + e_4^2\right) \tag{25}$$

here, $k_q > 0$ and $\log(\bullet)$ denotes the natural logarithm. BLFs are chosen for the first three components of output error that require a strict enforcement of constraints. Note that the Lyapunov function V_q is positive definite and C^1 continuous in the set $\mathcal{U}_{q_e}$. Further, the value of V_q is equal to zero only when $\mathcal{B}$ and $\mathcal{R}$ frames align with each other, i.e., when $e_1 = e_2 = e_3 = 0$ and $e_4 = 1$. The derivative of V_q is

$$\dot{V}_q = \boldsymbol{z}_q^T K_q Q_e \boldsymbol{\omega}_e - \frac{k_q}{2}\left(\sum_{i=1}^{3}\frac{\dot{\bar{e}}_i e_i}{\bar{e}_i(\bar{e}_i - e_i)}\right) \tag{26}$$

The vector $\boldsymbol{z}_q = [q_{1e}\ q_{2e}\ q_{3e}\ q_{4e} - 1]^T$ indicates the desired steady state tracking error of $\boldsymbol{q}_e$ and the matrix K_q is *diagonal* and positive definite in set $\mathcal{U}_{q_e}$ represented as

$$[K_q]_{1,1} = \frac{k_q}{\bar{e}_2 - e_2} + \frac{k_q}{\bar{e}_3 - e_3}, [K_q]_{2,2} = \frac{k_q}{\bar{e}_1 - e_1} + \frac{k_q}{\bar{e}_3 - e_3}$$
$$[K_q]_{3,3} = \frac{k_q}{\bar{e}_1 - e_1} + \frac{k_q}{\bar{e}_2 - e_2}, [K_q]_{4,4} = k_q$$

An angular velocity tracking error ($\boldsymbol{z}_\omega$) is defined as the difference between the relative angular velocity, $\boldsymbol{\omega}_e$ and a stabilizing function $\boldsymbol{\xi}$ as

$$\boldsymbol{z}_\omega = \begin{bmatrix} z_{\omega_1} & z_{\omega_2} & z_{\omega_3} \end{bmatrix}^T = \boldsymbol{\omega}_e - \boldsymbol{\xi} \tag{27}$$

The stabilizing function ($\boldsymbol{\xi}$) is designed as

$$\boldsymbol{\xi} = \left(-\tilde{k}_q - \bar{k}_q\right)\begin{bmatrix} q_{1e}/q_{4e} \\ q_{2e}/q_{4e} \\ q_{3e}/q_{4e} \end{bmatrix} \tag{28}$$

where, the constants $\bar{k}_q > 0$ and $\tilde{k}_q > 0$.

Remark 2: To ensure the validity of $\boldsymbol{\xi}$ in (28), the condition $q_{4e} \neq 0$ must be valid, $\forall\ t \ge 0$. Therefore, it is required to have a mild restriction on the initial condition such that $q_{4e}(t_0) \neq 0$, and the subsequent adaptive controller must be formulated to guarantee $q_{4e}(t) \neq 0$ for all time. This is feasible when the adaptive control law, $\boldsymbol{u}$, ensures the error quaternion to always lie within the feasible set $\mathcal{U}_{q_e}$, in which from Remark (1), $q_{4e} > 0$ is guaranteed.

Substituting (28), (27) into (26) simplifies $\dot{V}_q$ to

$$\dot{V}_q = -\frac{\tilde{k}_q k_q}{2}\left(\sum_{i=1}^{3}\frac{e_i}{\bar{e}_i - e_i}\right) - \frac{k_q\tilde{k}_q e_4^2\left(1+q_{4e}\right)}{2q_{4e}}\cdots + \boldsymbol{z}_\omega^T Q_e^T K_q \boldsymbol{z}_q + v_s \quad (29)$$

the scalar term v_s is denoted by the expression

$$v_s = \frac{-k_q\bar{k}_q e_4^2\left(1+q_{4e}\right)}{2q_{4e}} - \frac{k_q}{2}\sum_{i=1}^{3}\left(\bar{k}_q + \frac{\dot{\bar{e}}_i}{\bar{e}_i}\right)\left(\frac{e_i}{\bar{e}_i - e_i}\right) \quad (30)$$

Step 2: In this step the adaptive control law, $\boldsymbol{u}$, is designed. An augmented Lyapunov function is chosen as

$$V_T = V_q + V_\omega + V_b \quad (31)$$

where, V_q was defined in (25). The remaining Lyapunov functions are

$$V_\omega = \frac{\boldsymbol{z}_\omega^T J \boldsymbol{z}_\omega}{2},\ V_b = \frac{\tilde{\boldsymbol{b}}^T\tilde{\boldsymbol{b}}}{2\eta} \quad (32)$$

here, J indicates the moment of inertia matrix, $\tilde{\boldsymbol{b}}$ and $\eta > 0$ indicate the error in approximating the ideal weights and learning rate respectively. Consider the derivative of V_ω

$$\dot{V}_\omega = \boldsymbol{z}_\omega^T J\dot{\boldsymbol{z}}_\omega \quad (33)$$

Remark 3: Using (6) and (8), the following expression is obtained

$$J\dot{\boldsymbol{\omega}}_e = -\boldsymbol{\omega}^\times J\boldsymbol{\omega} + \boldsymbol{u} + \boldsymbol{\tau}_{ed} + J\left(\boldsymbol{\omega}_e^\times C_R^B\boldsymbol{\omega}_r - C_R^B\dot{\boldsymbol{\omega}}_r\right) \quad (34)$$

The uncertainty in the moment of inertia (J) is expanded in terms of the known (J_k) and unknown components (J_{uk}) as

$$J\dot{\boldsymbol{\omega}}_e = -\boldsymbol{\omega}^\times J_k\boldsymbol{\omega} - \boldsymbol{\omega}^\times J_{uk}\boldsymbol{\omega} + \boldsymbol{u} + \boldsymbol{\tau}_{ed}\cdots + J_k\left(\boldsymbol{\omega}_e^\times C_R^B\boldsymbol{\omega}_r - C_R^B\dot{\boldsymbol{\omega}}_r\right) + J_{uk}\left(\boldsymbol{\omega}_e^\times C_R^B\boldsymbol{\omega}_r - C_R^B\dot{\boldsymbol{\omega}}_r\right) \quad (35)$$

Using (35) and Lemma (3), the term $J\dot{\boldsymbol{z}}_\omega$ is expanded as

$$J\dot{\boldsymbol{z}}_\omega = J(\dot{\boldsymbol{w}}_e - \dot{\boldsymbol{\xi}}) = \boldsymbol{v}_k + \boldsymbol{u} + \boldsymbol{\tau}_{ed} + L\boldsymbol{\theta} \quad (36)$$

The vector $\boldsymbol{v}_k$ is defined as

$$\boldsymbol{v}_k = -\boldsymbol{\omega}^\times J_k\boldsymbol{\omega} + J_k\left(\boldsymbol{\omega}_e^\times C_R^B\boldsymbol{\omega}_r - C_R^B\dot{\boldsymbol{\omega}}_r\right) - J_k\dot{\boldsymbol{\xi}} \quad (37)$$

The matrix L multiplying the unknown moment of inertia vector $\boldsymbol{\theta}$ is

$$L = -\boldsymbol{\omega}^\times\mathcal{L}\{\boldsymbol{\omega}\} + \mathcal{L}\{\boldsymbol{\omega}_e^\times C_R^B\boldsymbol{\omega}_r - C_R^B\dot{\boldsymbol{\omega}}_r\} - \mathcal{L}\{\dot{\boldsymbol{\xi}}\} \quad (38)$$

The derivative of the total Lyapunov function in (31) is obtained using (29) and (36) as

$$\dot{V}_T = -\frac{\tilde{k}_q k_q}{2}\left(\sum_{i=1}^{3}\frac{e_i}{\bar{e}_i - e_i}\right) - \frac{k_q\tilde{k}_q e_4^2\left(1+q_{4e}\right)}{2q_{4e}} + v_s\cdots + \boldsymbol{z}_\omega^T\left(Q_e^T K_q\boldsymbol{z}_q + \boldsymbol{v}_k + \boldsymbol{u} + L\boldsymbol{\theta} + \boldsymbol{\tau}_{ed}\right) - \frac{\tilde{\boldsymbol{b}}^T\dot{\hat{\boldsymbol{b}}}}{\eta} \quad (39)$$

Using assumption (3) and property of dot product between two vectors, i.e., given $\boldsymbol{x},\boldsymbol{y} \in \mathbb{R}^n$, we have $\boldsymbol{x}^T\boldsymbol{y} \le \|\boldsymbol{x}\|_2\|\boldsymbol{y}\|_2$, the terms $\boldsymbol{z}_\omega^T L\boldsymbol{\theta}$ and $\boldsymbol{z}_\omega^T\boldsymbol{\tau}_{ed}$ in (39) satisfy

$$\boldsymbol{z}_\omega^T(L\boldsymbol{\theta} + \boldsymbol{\tau}_{ed}) \le \|\boldsymbol{z}_\omega\|_2\left(\|L\|_F\|\boldsymbol{\theta}\|_2 + \bar{\tau}_{ed}\right) \quad (40)$$

We define the ideal weights ($\boldsymbol{b}$) and regression vector ($\boldsymbol{\Phi}$) as

$$\boldsymbol{b} = \left[\|\boldsymbol{\theta}\|_2\ \bar{\tau}_{ed}\right]^T,\ \boldsymbol{\Phi} = \left[\|L\|_F\ 1\right]^T \quad (41)$$

Choosing the control and adaptive laws as

$$\boldsymbol{u} = -\tilde{k}_\omega\boldsymbol{z}_\omega - Q_e^T K_q\boldsymbol{z}_q - \boldsymbol{v}_k - \hat{\boldsymbol{b}}^T\boldsymbol{\Phi}\text{Tanh}\left(\frac{\boldsymbol{z}_\omega}{\varphi}\right) \quad (42)$$

$$\dot{\hat{\boldsymbol{b}}} = \eta\left(\boldsymbol{\Phi}\boldsymbol{z}_\omega^T\text{Tanh}\left(\frac{\boldsymbol{z}_\omega}{\varphi}\right) - \sigma\hat{\boldsymbol{b}}\right), \varphi = \mu/(1 + \|\boldsymbol{\Phi}\|_\infty) \quad (43)$$

here, $\hat{\boldsymbol{b}} = \boldsymbol{b} - \tilde{\boldsymbol{b}}$ represents the approximated weight vector with $\sigma, \mu > 0$. The notation $\text{Tanh}(\bullet) \in \mathcal{R}^3$ represents element-by-element hyperbolic tangent function as

$$\text{Tanh}\left(\frac{\boldsymbol{z}_\omega}{\varphi}\right) = \left[\tanh\left(\frac{z_{\omega_1}}{\varphi}\right)\quad \tanh\left(\frac{z_{\omega_2}}{\varphi}\right)\quad \tanh\left(\frac{z_{\omega_3}}{\varphi}\right)\right]^T \quad (44)$$

As long as the error quaternion lies within the feasible set $\mathcal{U}_{q_e}$, we have $q_{4e} > 0$. Consequently following observations are deduced in (30)

1) $(1 + q_{4e})/q_{4e} \ge 1$
2) The constant $\bar{k}_q$ in v_s is designed as a time-varying quantity such that $\bar{k}_q + \dot{\bar{e}}_i/\bar{e}_i > 0$ for $i = 1, 2, 3$. One possible value that satisfies the criterion is

$$\bar{k}_q = \sqrt{\frac{\dot{\bar{e}}_1^2}{\bar{e}_1^2} + \frac{\dot{\bar{e}}_2^2}{\bar{e}_2^2} + \frac{\dot{\bar{e}}_3^2}{\bar{e}_3^2} + k_\delta},\ k_\delta > 0 \quad (45)$$

In the above equation, k_δ is introduced to ensure the derivative of $\bar{k}_q$ in $\dot{\boldsymbol{\xi}}$ exists despite the derivative of output error constraints ($\dot{\bar{e}}_i,\ i = 1, 2, 3$) are all zero. The aforementioned observations lead to the scalar $v_s \le 0$ within the feasible set $\mathcal{U}_{q_e}$. Further, applying Lemma (1), Lemma (2) and substituting (40), (42) and (43), the Lyapunov derivative in (39) is

$$\dot{V}_T \le -\tilde{k}_q V_q - \tilde{k}_\omega\boldsymbol{z}_\omega^T\boldsymbol{z}_\omega + \sigma\tilde{\boldsymbol{b}}^T\hat{\boldsymbol{b}}\cdots + \boldsymbol{b}^T\boldsymbol{\Phi}\sum_{i=1}^{3}\left(|z_{\omega_i}| - z_{\omega_i}\tanh\left(z_{\omega_i}/\varphi\right)\right) \quad (46)$$

Using Lemma (2) on the term $\tilde{\boldsymbol{b}}^T\hat{\boldsymbol{b}}$, along with applying Lemma (4) and the inequality $\Phi_i/\left(1 + \|\boldsymbol{\Phi}\|_\infty\right) \le 1$, the total Lyapunov derivative is

$$\dot{V}_T \le -\tilde{k}_q V_q - k_\omega\boldsymbol{z}_\omega^T\boldsymbol{z}_\omega - \sigma\frac{\tilde{\boldsymbol{b}}^T\tilde{\boldsymbol{b}}}{2}\cdots + \sigma\frac{\boldsymbol{b}^T\boldsymbol{b}}{2} + 3\alpha\mu\left(\|\boldsymbol{\theta}\|_2 + \bar{\tau}_{ed}\right) \quad (47)$$

Further, applying the Rayleigh-Ritz inequality from Lemma (2), (47) reduces to

$$\dot{V}_T \le -k_v V_T + k_c \quad (48)$$

here, $k_v := \min\{\tilde{k}_q, 2k_\omega/\lambda_{\max}(J), \sigma\eta\} > 0$ and $k_c := \sigma\frac{\boldsymbol{b}^T\boldsymbol{b}}{2} + 3\alpha\mu\left(\|\boldsymbol{\theta}\|_2 + \bar{\tau}_{ed}\right) > 0$.

B. Stability Analysis

Theorem 1: Consider the reference tracking error dynamics described using (5) and (6) subjected to time varying output constraints in (11), (12) and (13) while satisfying assumptions (1), (2) and (3). Under the application of the control and adaptive laws in (42) and (43), the following properties hold.

1) Without parametric uncertainties and external disturbance torque, $\mathcal{B}$ asymptotically tracks $\mathcal{R}$ while strictly satisfying output constraints.
2) In the presence of modeling uncertainties and bounded external disturbances, the output errors $e_i(t),\ i = 1,2,3,4$ remain in the compact set defined by

$$\chi_{e_i} := \{e_i \in \mathbb{R} : e_i \leq \bar{e}_i \left(1 - e^{\frac{-2\bar{V}_T}{k_q}}\right)\}, i = 1,2,3$$

$$\chi_{e_4} := \{e_4 \in \mathbb{R} : e_4 \leq \sqrt{2\bar{V}_T/k_q}\}$$

whose sizes can be adjusted by properly choosing the design parameters. Further, the output errors $e_i(t),\ i = 1,2,3$ evolve strictly within $\mathcal{U}_{q_e}$ and the condition, $q_{4e} \neq 0$, remains valid for $t \geq 0$.

Proof 1: The solution to differential inequality in (48) is

$$V_T(t) \leq V_T(t_0)e^{-k_v t} + \frac{k_c}{k_v}\left(1 - e^{-k_v t}\right) \tag{49}$$

1) Without parametric uncertainties and external disturbance torques, i.e., with $k_c = 0$, (49) results in $V_T(t) \leq V_T(0)e^{-k_v t}$. As $k_v > 0$, the Lyapunov function $V_T(t) \to 0$ as $t \to \infty$ and is upper bounded by the value $V_T(t_0)$. Using the definition of V_T in (31), it can be concluded that $V_q(t) \to 0$ and $V_\omega(t) \to 0$ as $t \to \infty$. The definition of $V_q(t)$ and $V_\omega(t)$ in (25) and (32) ensures the output errors $e_i(t) \to 0,\ i = 1,2,3,4$ and $\boldsymbol{z}_\omega \to \boldsymbol{0}_{3\times 1}$ as $t \to \infty$. This implies the rigid-body asymptotically tracks the moving reference frame. Furthermore, $V_q(t) \leq V_T(t) \leq V_T(t_0)$ implies

$$e_i \leq \bar{e}_i \left(1 - \exp\frac{-2V_T(t_0)}{k_q}\right),\ i = 1,2,3 \tag{50}$$

Therefore the output errors strictly satisfy $e_i < \bar{e}_i\ \forall t > t_0,\ i = 1,2,3$ and hence stay within the set $\mathcal{U}_{q_e}$.
2) In the presence of modeling uncertainties and external disturbances both $k_v > 0$ and $k_c > 0$. From (49), the Lyapunov function $V_T(t)$ is upper bounded by $\bar{V}_T = V_T(t_0) + \frac{k_c}{k_v}$. The definition of $V_T(t)$ in (31) results in the following inequalities

$$e_i \leq \bar{e}_i \left(1 - \exp\frac{-2\bar{V}_T}{k_q}\right),\ i = 1,2,3, e_4 \leq \sqrt{\frac{2\bar{V}_T}{k_q}} \tag{51}$$

$$\|\boldsymbol{z}_\omega\| \leq \sqrt{2\bar{V}_T/\lambda_{max}(J)},\ \|\tilde{b}\| \leq \sqrt{2\eta\bar{V}_T} \tag{52}$$

From (51), it is obsverved that the output errors satisfy the constraint $e_i < \bar{e}_i \forall t > t_0, i = 1,2,3$ thereby strictly remaining within $\mathcal{U}_{q_e}$, in which $q_{4e} \neq 0$. Further, notice from (49), as $t \to \infty$, we have $V_T(t_\infty) \leq \frac{k_c}{k_v}$. Using a similar analysis, the steady state errors are shown to be uniformly ultimately bounded (UUB) as

$$e_i(t_\infty) \leq \bar{e}_i(t_\infty)\left(1 - \exp\frac{-2k_c}{k_q k_v}\right),\ i = 1,2,3 \tag{53}$$

From (51) and (52), we have $q_{ie}, \forall i = 1,2,3,4$ and $\boldsymbol{z}_\omega$ to be bounded quantities. This implies $\boldsymbol{\xi}$ in (28), $\boldsymbol{\omega}_e$ in (27) and $\boldsymbol{\omega}$ in (3) are bounded quantities. Therefore, all the closed loop signals are bounded.

V. Numerical simulation and Discussion

Let, at t_0, the rigid-body frame ($\mathcal{B}$) is oriented to the inertial frame ($\mathcal{I}$) via a $3-2-1$ Euler angle sequence of $(0^\circ) - (0^\circ) - (90^\circ)$. At the same time, the reference frame ($\mathcal{R}$) is aligned to $\mathcal{I}$ and has an angular velocity $\boldsymbol{\omega}_r = -0.2\,\hat{r}_1$ deg/s. The resulting reference quaternion profile is

$$q_{1r} = -\sin\frac{\omega_r t}{2},\ q_{2r} = 0,\ q_{3r} = 0,\ q_{4r} = \cos\frac{\omega_r t}{2} \tag{54}$$

here, $\omega_r = 0.2$ deg/s. It is straightforward to verify that the initial relative attitude error between $\mathcal{B}$ and $\mathcal{R}$ frames, that are denoted by the angles between $\hat{b}_i$ and $\hat{r}_i$ axes are $\delta_1(t_0) = 0^\circ$, $\delta_2(t_0) = 90^\circ$ and $\delta_3(t_0) = 90^\circ$ respectively. In addition to aligning $\mathcal{B}$ and $\mathcal{R}$ frames, the adaptive controller must ensure that the relative attitude errors evolve within a prescribed performance cone angles $\bar{\delta}_i(t),\ i = 1,2,3$ given as

$$\bar{\delta}_i(t) = \bar{\delta}_i(t_\infty) + \left(\bar{\delta}_i(t_0) - \bar{\delta}_i(t_\infty)\right)e^{-\frac{t-t_0}{t_c}} \tag{55}$$

here, for $i = 1,2,3$, the constants are chosen as $\bar{\delta}_i(t_0) = 91^\circ$, $\bar{\delta}_i(t_\infty) = 0.5^\circ$ and $t_c = 40$ sec. The selection of the cone angle constraints in (55) ensures assumption (2) and (16) are satisfied. The rigid body has a known moment of inertia matrix $J_k = \mathrm{diag}(100, 80, 120)\ kg - m^2$. The performance of the adaptive control law is tested in the presence of moment of inertia uncertainty and an unknown bounded disturbance. Each element of the unknown moment of inertia matrix (J_{uk}) is perturbed by a value of $\pm 20\ kg - m^2$. Note that there are six independent elements that can be varied in J_{uk}. The rigid body is subjected to time-varying bounded disturbance torque

$$\boldsymbol{\tau}_{ed} = 5 \times 10^{-4}\begin{bmatrix}\pm(\cos\omega_t t + \sin\omega_t t + 10)\\ \pm(\cos\omega_t t - \sin\omega_t t + 10)\\ \pm(-\cos\omega_t t + \sin\omega_t t + 10)\end{bmatrix} N - m$$

here $\omega_t = 0.01\ rad/s$. The sign of the disturbance torque is independently varied across the three channels. Overall, the adaptive controller is tested for 2^9 disturbance variations. The adaptive controller parameters are listed in Table (I). First, the evolution of attitude errors (δ_i) using an unconstrained controller is shown in Fig. (2). Note that a conventional quadratic Lyapunov function (QLF) $V_q = \Sigma_{i=1}^4 e_i^2$ with $e_i = q_{ie} - 0$ for $i = 1,2,3$ and $e_4 = q_{4e} - 1$ is chosen in the place of (25), while the rest of control synthesis including controller constants remain the same. Although all the initial attitude errors lie within the error bounds, after a certain time, the attitude errors violate the performance bounds during the transient as well as steady state behaviour. The effectiveness of the adaptive,

Table I: Controller Parameters

Constant	k_q	$\tilde{k}_q$	$\bar{k}_q$	$\tilde{k}_\omega$
Value	5.4×10^{-4}	5.4×10^{-2}	$\sqrt{\frac{\dot{\bar{e}}^2}{\bar{e}^2} + k_\delta}$	2.6×10^{0}
Constant	k_δ	η	σ	μ
Value	5.0×10^{-5}	6.0×10^{-2}	1.0×10^{-6}	1.0×10^{0}

BLF based controller in shown in Fig. (3). Under various combinations of disturbance, the $\mathcal{B}$ frame is driven to $\mathcal{R}$ while strictly remaining within the attitude error bounds. The steady state errors settle below $\bar{\delta}_i(t_\infty)$ for $i = 1, 2, 3$.

Figure (4) showcases a particular scenario in more detail. Using an adaptive, BLF based controller in Fig. (4), the $\bar{\delta}_i - \delta_i$ plot always stays positive, indicating that attitude constraints are respected for all time. Finally, the disturbance estimate ($\hat{d}$) together with the actual disturbance (d) is shown on the left in Fig. (5). Notice, that the disturbance estimate starts at zero and eventually approximates the actual disturbance profile. The adaptive control profile across the three channels is indicated on the right. The control profile is smooth and settles at a non-zero value to negate the continuous disturbance torque.

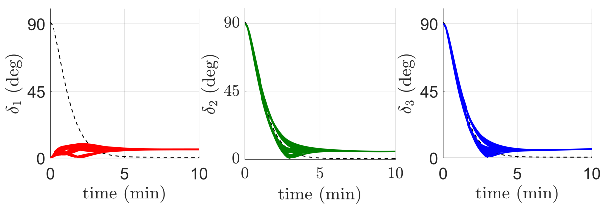

Figure 2: Attitude error evolution under uncertainties and disturbances using a nominal QLF based controller.

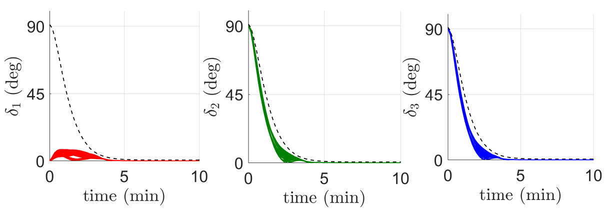

Figure 3: Attitude error evolution under uncertainties and disturbances using an adaptive BLF based controller.

VI. Conclusion

In this paper, a BLF based adaptive control law is designed using backstepping to handle time-varying attitude constraints. First, the orientation error between the rigid-body and the desired frame is defined using a set of cone angles. Using an appropriate error transformation, the attitude constraints on the cone angles are converted into quaternion constraints. Subsequently Lyapunov analysis is carried out to obtain a robust, adaptive controller capable of tracking the reference frame and simultaneously avoiding the transgression

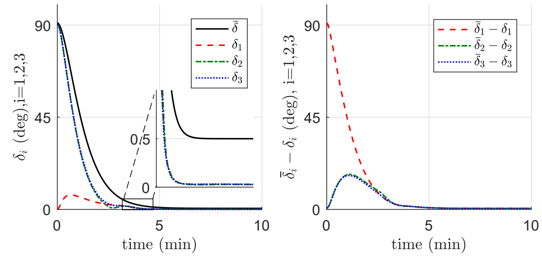

Figure 4: Attitude error evolution using a BLF based adaptive controller.

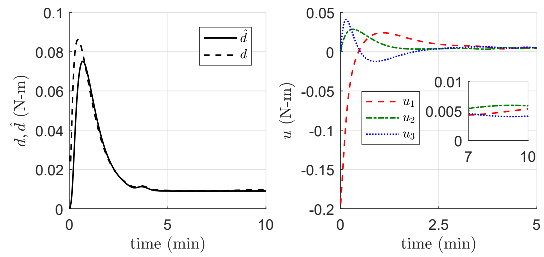

Figure 5: Disturbance estimation and adaptive control profile.

of attitude constraints. Finally, in the presence of parametric uncertainties and bounded disturbances, numerical simulations and comparison with an attitude control law derived using conventional QLFs is provided to illustrate the effectiveness of the proposed controller.

References

[1] J. Yang and E. Stoll, "Time-optimal spacecraft reorientation with attitude constraints based on a two-stage strategy," in *Proceedings of the AAS/AIAA Astrodynamics Specialist Conference, AAS*, 2018, pp. 18–201.

[2] J. Wang and H. Shang, "Constrained spacecraft attitude optimal control via successive convex optimization," in *Journal of Physics: Conference Series*, vol. 2095, no. 1. IOP Publishing, 2021, p. 012039.

[3] M. Diaz Ramos and H. Schaub, "Kinematic steering law for conically constrained torque-limited spacecraft attitude control," *Journal of Guidance, Control, and Dynamics*, vol. 41, no. 9, pp. 1990–2001, 2018.

[4] Q. Hu, Y. Liu, H. Dong, and Y. Zhang, "Saturated attitude control for rigid spacecraft under attitude constraints," *Journal of Guidance, Control, and Dynamics*, vol. 43, no. 4, pp. 790–805, 2020.

[5] Q. Hu, X. Shao, and L. Guo, "Adaptive fault-tolerant attitude tracking control of spacecraft with prescribed performance," *IEEE/ASME Transactions on Mechatronics*, vol. 23, no. 1, pp. 331–341, 2017.

[6] C. Wei, Q. Chen, J. Liu, Z. Yin, and J. Luo, "An overview of prescribed performance control and its application to spacecraft attitude system," *Proceedings of the Institution of Mechanical Engineers, Part I: Journal of Systems and Control Engineering*, vol. 235, no. 4, pp. 435–447, 2021.

[7] K. P. Tee, S. S. Ge, and E. H. Tay, "Barrier lyapunov functions for the control of output-constrained nonlinear systems," *Automatica*, vol. 45, no. 4, pp. 918–927, 2009.

[8] H. J. Marquez, *Nonlinear control systems: analysis and design*. Wiley-Interscience Hoboken, NJ, 2003, vol. 1.

[9] S. Vutukuri and R. Padhi, "Quaternion constrained robust attitude control using barrier lyapunov function based back-stepping," *IFAC-PapersOnLine*, vol. 55, no. 1, pp. 522–527, 2022.

[10] F. L. Markley and J. L. Crassidis, "Fundamentals of spacecraft attitude determination and control," 2014.

[11] K. P. Tee, B. Ren, and S. S. Ge, "Control of nonlinear systems with time-varying output constraints," *Automatica*, vol. 47, no. 11, pp. 2511–2516, 2011.